Dynamics in molecular and molecular–ionic crystals: A combined experimental and molecular simulation study of reorientational motions in benzene, pyridinium iodide, and pyridinium…

ARTICLE *in* THE JOURNAL OF CHEMICAL PHYSICS · JANUARY 2013

Impact Factor: 2.95 · DOI: 10.1063/1.4774096 · Source: PubMed

3 AUTHORS, INCLUDING:

Aleksandra Pajzderska

Adam Mickiewicz University

45 PUBLICATIONS **141** CITATIONS

SEE PROFILE

Dynamics in molecular and molecular-ionic crystals: A combined experimental and molecular simulation study of reorientational motions in benzene, pyridinium iodide, and pyridinium nitrate

A. Pajzderska, M. A. Gonzalez, and J. Wąsicki

Citation: J. Chem. Phys. **138**, 024508 (2013); doi: 10.1063/1.4774096
View online: http://dx.doi.org/10.1063/1.4774096
View Table of Contents: http://jcp.aip.org/resource/1/JCPSA6/v138/i2
Published by the American Institute of Physics.

Dynamics in molecular and molecular-ionic crystals: A combined experimental and molecular simulation study of reorientational motions in benzene, pyridinium iodide, and pyridinium nitrate

A. Pajzderska,[1] M. A. Gonzalez,[2] and J. Wąsicki[1]
[1]*Faculty of Physics, A. Mickiewicz University, Poznań, Poland*
[2]*Institute Laue Langevin, B.P. 156x, 38042 Grenoble Cedex 9, France*

(Received 2 August 2012; accepted 18 December 2012; published online 11 January 2013)

Molecular dynamics (MD) simulations for crystalline benzene (C_6H_6), pyridinium iodide $[C_5NH_6]^+I^-$, and pyridinium nitrate $[C_5NH_6]^+NO_3^-$ have been performed as a function of temperature and pressure. Despite the similar shape of the benzene molecule and the pyridinium cation, the experimental and simulated data have showed clear differences in their dynamics. Therefore, the rotational dynamics have been explored in detail by comparing thoroughly the existing experimental results together with new quasielastic neutron scattering (QENS) data obtained for $(PyH)NO_3$ and molecular dynamics simulations. The correlation times, activation energy, geometry of motion of benzene molecule and pyridinium cation, isothermal compressibility, and activation volume obtained from the simulations are compared with the experimental results obtained by nuclear magnetic resonance and QENS methods. MD simulations have also revealed that reorientation of the pyridinium cation in pyridinium nitrate between two inequivalent positions is strongly affected by the hydrogen bond N–H$\cdots$O between the cation and the anion and the influence of temperature on strength of the hydrogen bond is much more important than that of the pressure. © *2013 American Institute of Physics*. [http://dx.doi.org/10.1063/1.4774096]

I. INTRODUCTION

Simple pyridinium salts are ion-molecular systems showing a number of interesting physicochemical properties. The planar pyridinium cation has a dipole moment and the possible anions may have different shapes: spherical in pyridinium bromide[1] and pyridinium iodide (hereafter (PyH)I),[1,2] planar in pyridinium nitrate ((PyH)NO_3),[3,4] tetrahedral in pyridinium tetrafluoroborate,[1,5,6] pyridinium perchlorate,[7,8] pyridinium periodate,[9] and pyridinium perherate[10], and octahedral in pyridinium hexafluorophosphate[11,12] and pyridinium hexafluoroantimonate.[13] All these salts except pyridinium nitrate present at least one phase transition. The pyridinium salts with anions of tetrahedral shape undergo two phase transitions and the low-temperature phase and the intermediate phase of pyridinium tetrafluoroborate,[6] pyridinium perchlorate,[7] pyridinium perherate,[10] and the intermediate phase of pyridinium periodate[10] show ferroelectric ordering. In all pyridinium salts studied up to now, the reorientations of the pyridinium cation in the low-temperature or intermediate phases take place between potential minima having different energies (asymmetric potential and after the transition to the high-temperature phase the potential becomes symmetric and the pyridinium cations reorient between equivalent potential energy minima). Much effort has been made to prove that the pyridinium cation really reorients in a temperature dependent asymmetric potential, as such potential allows describing the ferroelectric properties of these compounds. Thus, the compounds pyridinium iodide,[2,14–16] pyridinium tetrafluoroborate,[17] pyridinium perchlorate,[18,19] pyridinium periodate,[20–22] pyridinium perherate,[23,24] and pyridinium nitrate[4] have been studied by ^{1}H nuclear magnetic resonance (NMR) and inelastic neutron scattering as a function of temperature and pressure and by ^{2}H NMR and quasielastic neutron scattering (QENS) as a function of temperature. A detailed analysis of the dynamics of molecules or ions provides important information to understand their properties or the mechanism of their phase transitions. In the case of ion-molecular crystals particularly interesting data can be obtained from the analysis of the molecular reorientations of the cationic and anionic sublattices. For pyridinium salts, reorientations of both ionic sublattices could be studied by NMR and the results revealed a very interesting convergence of the rotational correlation times of cations and anions at the phase transition. Such effect has been observed for pyridinium tetrafluoroborate,[5] pyridinium hexafluorophosphate,[11,12] and pyridinium hexafluoroantimonate.[13] Unfortunately, the experimental determination of the correlation time has not been achievable for all anions, so it is not possible to check if this effect takes place in all pyridinium salts. However, a similar effect of convergence of rotational correlation times of cations and anions has been observed for two guanidine salts: tetrafluoroborate[25] and hexafluorophosphate.[26]

From the above compounds, we have chosen to study in detail the rotational dynamics of two pyridinium salts—pyridinium iodide and nitrate—which have anions of different shapes (spherical iodide and planar nitrate anions, respectively) and crystalline benzene as a reference compound. Pyridinium iodide undergoes a phase transition at 247 K.[15] The high temperature phase (PyH)I crystallizes in the rhombohedral system, space group $R\bar{3}m$,[27] while the structure of the low-temperature phase is unknown. In contrast, in pyridinium

nitrate there is no phase transition up to the melting point (390 K) and (PyH)NO_3 crystallizes in the monoclinic system, space group $P2_1/c$.[28] The structure of crystalline benzene is also well known, being orthorhombic, space group Pbca.[29]

Despite the similar shape of the benzene molecule and the pyridinium cation, the experimental data show clear differences in their dynamics. Benzene molecules and pyridinium cations in the high temperature phase of (PyH)I) reorient between six equivalent minima.[15,16,30] However, in the low-temperature phase, the pyridinium cation jumps between potential minima having different energies. Finally, in the case of the pyridinium cation in (PyH)NO_3 its reorientation takes place between non-equivalent positions—at all temperatures studied. Previous experimental results have been interpreted assuming that the heights of the rotational potential barriers for the pyridinium cation in (PyH)NO_3 and the low-temperature phase of (PyH)I are temperature dependent.[3,14] In the present work, we intend to explore in detail such assumption by comparing thoroughly the existing experimental results together with new QENS data obtained for (PyH)NO_3 and molecular dynamics (MD) simulations. The later have been performed for the three compounds—benzene, (PyH)I, and (PyH)NO_3—as a function of temperature and pressure. While both physical parameters play an extremely important role in determining the structure and dynamics of organic molecular crystals, the effect of pressure is still relatively poorly understood.

II. EXPERIMENTAL DETAILS

We have performed QENS measurements on a polycrystalline sample of pyridinium nitrate on the backscattering spectrometers IN10 at 260 K at the Institute Laue-Langevin, Grenoble. The incident wavelength was 6.27 Å and the energy resolution of the instrument is 0.9 μeV (FWHM). The energy and Q-ranges covered are ± 15 μeV and 0.2–1.96 $Å^{-1}$, respectively.

The sample was prepared as described in Ref. 3 and was placed in an aluminium flat slab holder of size 4 × 3 cm^2 of thickness 0.3 mm giving a transmission coefficient of 0.9, so multiple scattering corrections can be neglected. The angle between the sample surface and the incident neutron beam was 135°. Raw data were treated with the LAMP program,[31] which was used to subtract the background using a measurement of the empty container taking into account sample absorption. Then, using a vanadium spectrum as an elastic scattering standard the intensities were normalized in order to correct for different detector efficiencies.

The spectra obtained in this way can then be fitted with the following model-independent function:[32,33]

$$S_{inc}(Q,\omega) = e^{-2W(Q)}\left[A_0(Q)\delta(\omega) + (1-A_0)\,L(\omega)\right] \otimes R(Q,\omega) + B(Q), \quad (1)$$

where $e^{-2W(Q)}$is the Debye-Waller factor, $A_0(Q)\delta(\omega)$ represents the purely elastic part, $(1 - A_0)L(\omega)$ gives the total quasielastic contribution, $L(\omega)$ is a Lorentzian function with width $\Gamma(Q, T)$, $R(Q, \omega)$ is the resolution function, and $\otimes$ means the convolution.

III. CALCULATION DETAILS

MD simulations have been performed with the DL_POLY 2.20 package[34] for three compounds: benzene, pyridinium iodide, and nitrate.

The simulation boxes were constructed on the basis of the X-ray crystallographic data[27–29] and consist of 100, 216, and 90 unit cells, their dimensions were equal to 37.3 × 38.664 × 35.17 $Å^3$, 33.2262 × 33.2262 × 33.2262 $Å^3$, 37.756 × 37.008 × 40.059 $Å^3$ and contain 400 benzene molecules, 216 pyridinium cations and iodide anions, and 360 pyridinium cations and nitrate anions for benzene, (PyH)I, and (PyH)NO_3, respectively.

All simulations were performed in the *NPT* ensemble as a function of temperature and pressure. Periodic boundary conditions were applied and the temperature and pressure were controlled using Berendsen's thermostat and barostat with relaxation constants of 1 ps and 5 ps, respectively. A cutoff distance of 15.5 Å (benzene, (PyH)I) or 17.5 Å ((PyH)NO_3) was applied for the Van der Waals forces and the electrostatic interactions were treated using the Ewald summation method with the same cutoff in real space. In all cases, a time step of 1 fs was used and the systems were equilibrated during 500 ps. Then the trajectory was saved every 1.5 ps for a total simulation time of 5 ns for benzene and pyridinium iodide and every 2.5 ps for a total simulation time of 10 ns for pyridinium nitrate. The time-lengths of the simulations are sufficiently long compared to the characteristic times probed by conventional backscattering QENS spectrometers and/or NMR experiment. Benzene molecules, pyridinium cations, and nitrate anions were treated as rigid bodies.

For benzene and (PyH)I, the interaction energy was described using the Lennard-Jones and electrostatic terms, while for (PyH)NO_3 an additional hydrogen-bond term of the form

$$V_{ij}^{HB}(r_{ij}) = \frac{A_{ij}}{r_{ij}^{12}} - \frac{B_{ij}}{r_{ij}^{10}} \quad (2)$$

was included. All the Lennard-Jones and hydrogen-bond parameters employed were taken from Refs. 35 and 36.

The charge distribution was obtained from a Mulliken population analysis performed over the electronic structure obtained from a density functional theory (DFT) calculation on a supercell of one unit cell of benzene, pyridinium iodide and nitrate. The DFT calculation was done with the DMol^3 module in Materials Studio,[37] using the GGA-BLYP functional, a single Γ point, and including all the core electrons in the calculation. The final charges employed in the MD simulations are summarized in the Table I.

As a first test of the force field, we simulated the three crystals at ambient pressure and the temperatures corresponding to the crystallographic data reported in Refs. 27–29 finding that the relative differences between the experimental and simulated unit cell lengths are less than 2% for benzene and pyridinium nitrate and about 4% for pyridinium iodide.

TABLE I. Charges used in the simulations for benzene, pyridinium iodide, and pyridinium nitrate. Numbering of atoms is the same as in Fig. 1.

	q_i [e]		
Atom	Benzene	(PyH)I cation	$(PyH)NO_3$ cation
C1/N	− 0.155	− 0.429	− 0.401
H1	0.154	0.382	0.424
C2	− 0.180	− 0.020	0.036
H2	0.171	0.265	0.246
C3	− 0.165	− 0.205	− 0.159
H3	0.175	0.254	0.221
C4	− 0.155	− 0.154	− 0.126
H4	0.154	0.254	0.197
C5	− 0.180	− 0.205	− 0.159
H5	0.171	0.254	0.221
C6	− 0.165	− 0.020	0.036
H6	0.175	0.265	0.246
Atom	(PyH)I anion	Atom	$(PyH)NO_3$ anion
I	− 0.641	N	0.676
		O	− 0.486
		O	− 0.486
		O	− 0.486

IV. RESULTS AND DISCUSSION

A. Simulations in a function of temperature

1. Benzene and pyridinium iodide

In order to analyze the reorientations of the benzene molecule and pyridinium cation, the following vectors were defined: $\mathbf{r}_1$ as the one crossing the two opposite carbon atoms (for benzene) and the nitrogen and carbon atoms (for pyridinium cation) and $\mathbf{r}_2$ as the one perpendicular to the plane of the molecule or cation (Fig. 1). Then the angle Θ made by the vectors $\mathbf{r}_1(t = 0)$ and $\mathbf{r}_1(t)$ and the angle φ made by the vectors $\mathbf{r}_2(t = 0)$ and $\mathbf{r}_2(t)$ were calculated as functions of time. The value of φ as a function of time fluctuates only slightly around 0°, indicating that the molecule of benzene and the pyridinium cation do not perform out-of-plane motions.

In Figs. 2(a) and 2(b), we show the typical behaviour of Θ(t) for a selected molecule of benzene and pyridinium in (PyH)I at 270 K and 300 K, respectively. In both cases, there

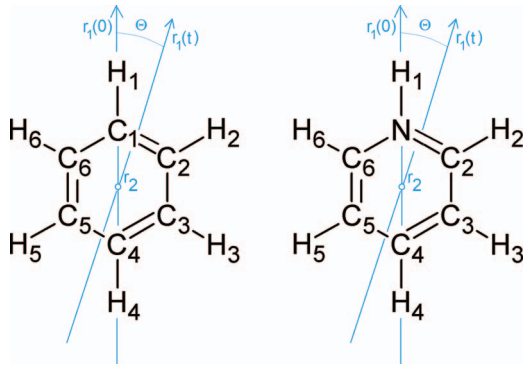

FIG. 1. The sketch of benzene molecule (left) and pyridinium cation (right). The vector $\mathbf{r}_1$ lies in molecular plane and pass through opposite atom and $\mathbf{r}_2$ is perpendicular to the plane.

are six well-distinguished positions distanced by 60°. Global information on the geometry of the reorientations is obtained from the orientation distribution function $P(\Theta)$ defined as

$$P(\Theta) = \frac{1}{N_{mol}} \frac{1}{N_{step}} \sum_{i}^{N_{step}} N(\Theta, \Theta + d\Theta), \tag{3}$$

where N_{mol} is the number of benzene molecules or pyridinium cations in the simulation box, $N(\Theta, \Theta + d\Theta)$ is the number of molecules/cations found with an orientation in the range $(\Theta, \Theta + d\Theta)$, and the summation is performed over all molecules/cations N_{mol} and all time steps N_{step}.

This probability function $P(\Theta)$ is also shown in Fig. 2. For benzene and (PyH)I, it displays six maxima of similar amplitude for the angles of −120°, −60°, 0°, 60°, 120°, and 180°. Thus, the benzene molecule and the pyridinium cation can occupy six equilibrium positions. The same geometry of motion has been proposed earlier on the basis of NMR[15,38,39] and QENS data.[16,30]

As the QENS experiment is particularly sensitive to the geometry of motion, a stringent test of the simulations consist in comparing the experimental EISF ($EISF_{experim} = A_0(Q)$) with that extracted from the simulated trajectories ($EISF_{simulated}$). $EISF_{simulated}$ were calculated directly in nMoldyn[40] using the expression:[28] $\sum_i b_{i,inc}^2 \langle|\exp(i\vec{Q}\vec{R}_i)|^2\rangle / (\sum_i b_{i,inc}^2)$, where $b_{i,inc}$ is the incoherent scattering length of atom i. In that case, the simulated EISF ($EISF_{simulated}$) can be compared with the experimental EISF (=$A_0(Q)$) using the relation[41]

$$\begin{aligned} EISF_{simulated} &= \exp(-u^2Q^2) \cdot EISF_{experimental} \\ &= \exp(-u^2Q^2) \cdot A_0(Q), \end{aligned} \tag{4}$$

where u^2 is the vibrational mean square displacement, which was estimated as $\langle|(r_i(t) - r_i(0))|^2\rangle$ where $r_i(t)$ is the position of the molecular centre of mass at time t, and $r_i(0)$ is the initial position. From our simulations, we obtain u^2 equal to 0.66 Å^2 for benzene at 270 K and to 0.80 Å^2 for (PyH)I at 290 K.

As mentioned above QENS data for benzene and pyridinium iodide at different temperatures are available in the literature.[16,30] For benzene at 210 K, 246 K (Fig. 6), and 273 K and for (PyH)I at 296 K and 270 K (high temperature phase) the authors found that the QENS spectra are best fitted by a sixfold rotational model between equivalent sites on a circle of radius r in the molecular plane. In this model, the EISF is defined as[32]

$$A_0(Q) = \frac{1}{N} \sum_{n=1}^{N} j_0\left(2Qr \sin\frac{n\pi}{N}\right), \tag{5}$$

where j_0 is the zeroth-order spherical Bessel function and N is the number of equivalent positions. This EISF(=$A_0(Q)$) (using $N = 6$ and $r = 2.4$ Å) is shown in Fig. 3 as a solid line together with the points directly obtained from the simulation using Eq. (4). Clearly, the simulated EISF matches perfectly with the model used to fit the QENS data.

The other important parameter characterizing the motion is the characteristic correlation time. For the angle Θ(t) defined above, the following two autocorrelation functions (ACF) were calculated: $C_1(t) = \langle\cos(\Theta)\rangle$ and $C_2(t)$

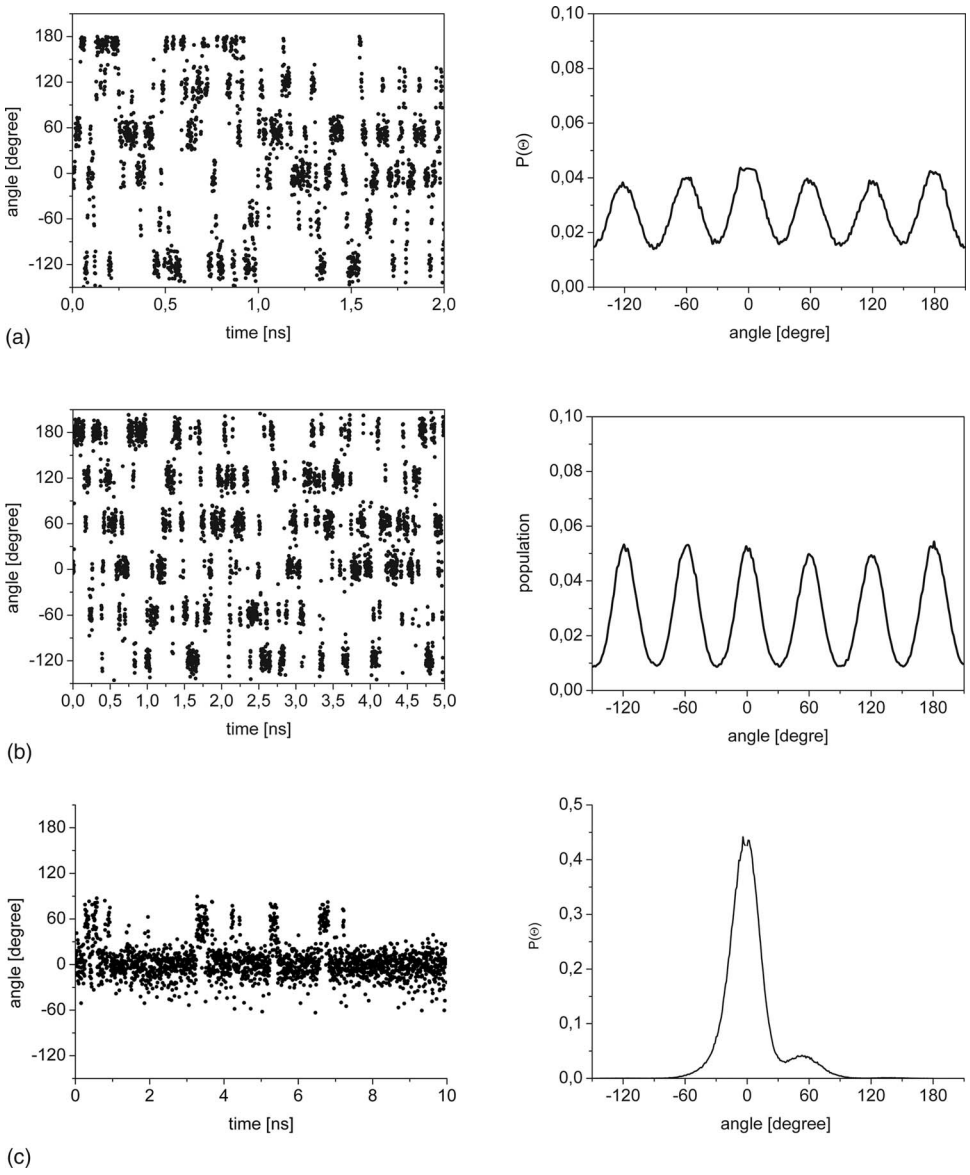

FIG. 2. Time evolution of Θ angle for selected molecule and/or pyridinium cation (left) and the total distribution function $P(\Theta)$ (right) for (a) benzene 270 K, (b) (PyH)I 290 K, (c) $(PyH)NO_3$ 290 K.

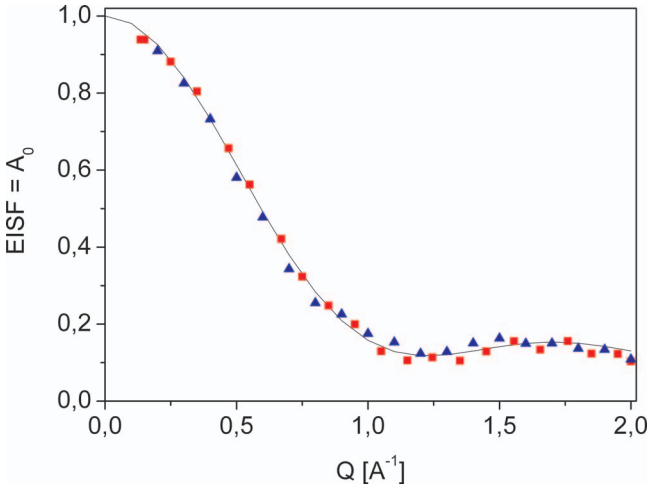

FIG. 3. Simulated EISF for benzene (▲) and (PyH)I (■) in comparison with the theoretical line corresponding to the model of jumps between 6 equivalent sites on a circle in the molecular plane calculated using Eq. (5).

$= \langle 0.5(3\cos^2(\Theta) - 1)\rangle$, corresponding to the Legendre polynomial of first and second order and each one was fitted to a single exponential in order to obtain the correlation times τ_1 and τ_2. Those times can be compared with the experimental data obtained from QENS measurements (for τ_1) or NMR measurements (for τ_2), as shown in Fig. 4. Again the agreement between simulation and experiment is very good. The activation energies deduced from the temperature dependence of the experimental and simulated correlation times are compared in Table II. The reasonable agreement between simulation and experiment validates the choice of the force field to model both molecular crystals.

Here, it is worth to mention that the MD simulations of (PyH)I as a function of temperature show a qualitative change below 200 K, as the picture of 6 equivalent minima in the rotational potential breaks. As shown in Fig. 5, one of the maxima of the $P(\Theta)$ distribution starts to be significantly more populated than the other five and this trend increases with

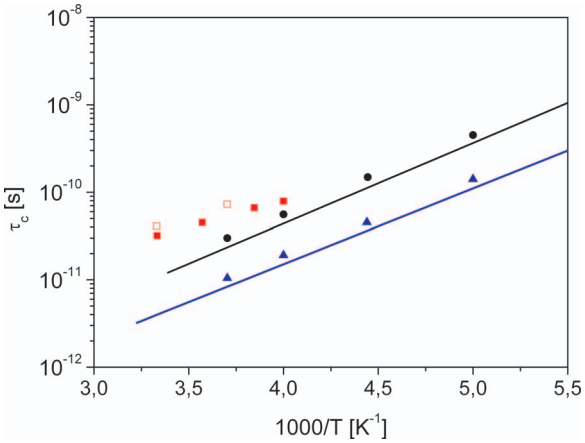

FIG. 4. Rotational correlation times for benzene (τ_2 from simulation (▲) and NMR experiments [Ref. 39] (blue solid line) extracted from $C_2(t)$ and τ_1 derived from the simulated correlation function $C_1(t)$ (●) and from QENS experiments [Ref. 30] (black solid line)) and for (PyH)I (τ_1 from simulation (■)and QENS [Ref. 16] (□)).

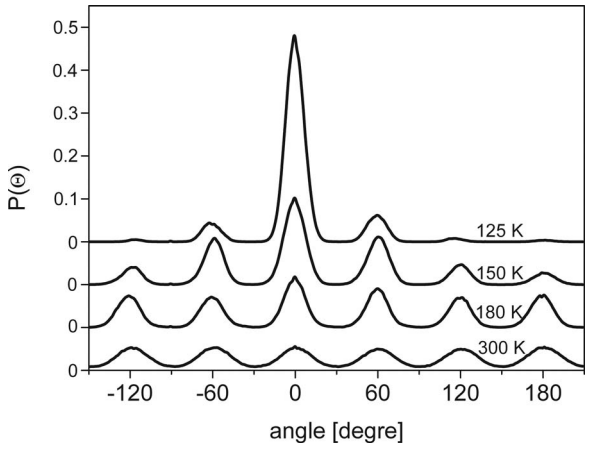

FIG. 5. The total distribution function $P(\Theta)$ for (PyH)I in a function of temperature.

decreasing temperature. This result implies that at low temperatures the reorientation of the pyridinium cation in (PyH)I takes place in an asymmetric potential. This implication is consistent with the results of the spin-lattice T_1 relaxation time measurements as a function of temperature[15] and pressure.[2]

The QENS results for (PyH)I in the low-temperature phase at 240 K[16] were interpreted as residual disorder of pyridinium cation. These data could also be well interpreted assuming the asymmetric potential of cation reorientation. Moreover, it has been shown that with increasing temperature the asymmetry of the potential is gradually reduced and at the phase transition temperature (250 K) the potential becomes symmetric.[14] As follows from the MD simulations, the potential asymmetry is related to the formation of a hydrogen bond N–H···I. However, the MD simulation results should be treated with caution as they were obtained from the high-temperature (PyH)I structure. Unfortunately, because of the lack of data on the low-temperature structure of this compound, we were not able to perform similar simulations for the low-temperature phase.

TABLE II. Experimental and simulated activation energies.

	Experimental	MD (kJ/mol) [this work]
Benzene	QENS 17.6 kJ/mol [obtained from Arrhenius plot in Ref. 30], NMR 15.5 ± 0.8 kJ/mol [Ref. 38], NMR 17.2 kJ/mol [Ref. 39], NMR 17.6 kJ/mol [Ref. 49]	16.9
Pyridinium cation ((PyH)I)	NMR 17.6 kJ/mol [Ref. 15], QENS 14.6 ± 2.9 kJ/mol [Ref. 16]	11.2

2. Pyridinium nitrate

The same kind of analysis was applied to the simulations of $(PyH)NO_3$. But as in this case we have a planar anion, the study was done on both the cation and the anion. In the case of the cation, again no out-of-plane motion was observed, as the angle φ only shows small fluctuations around 0°. However, the temperature dependence of $\Theta(\tau)$ is much different, as shown in Fig. 2(c). Now the cation assumes only two positions at 0° and 60° and the probability function $P(\Theta)$ presents a large maximum at 0° and a much smaller one at 60°.

As mentioned above, quasielastic neutron scattering is a very accurate method to investigate the geometry of motions at a microscopic scale. QENS measurements were made for $(PyH)NO_3$ at 260 K (Fig. 6). The spectra were fitted for all Q values using Eq. (1). The width of the quasielastic broadening is Q independent (within the error bars), as expected for a rotational motion between two or three positions. The correlation time τ estimated from the width of the Lorentzian function is shown in Fig. 10. From the data fit, we also obtain directly the elastic incoherent structure factor,

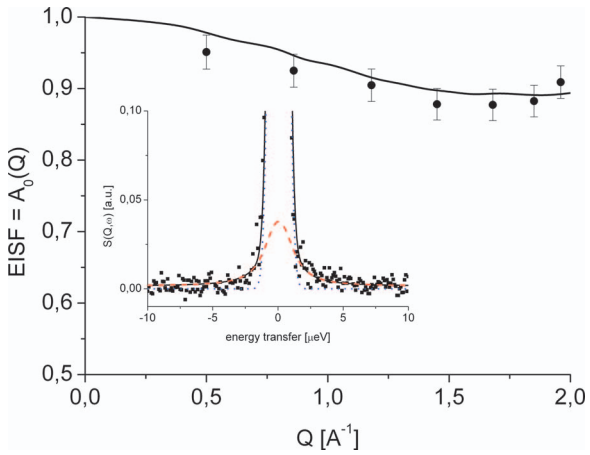

FIG. 6. Comparison experimental (■) elastic incoherent structure factor for the pyridinium cation in $(PyH)NO_3$ (EISF = $A_0(Q)$) and simulated EISF (———). (Inset) QENS normalized spectra at Q = 1.68 $Å^{-1}$. The solid black line shows the fitted spectra, the dotted blue line corresponds to the resolution function, and the dashed red line is the quasielastic contribution.

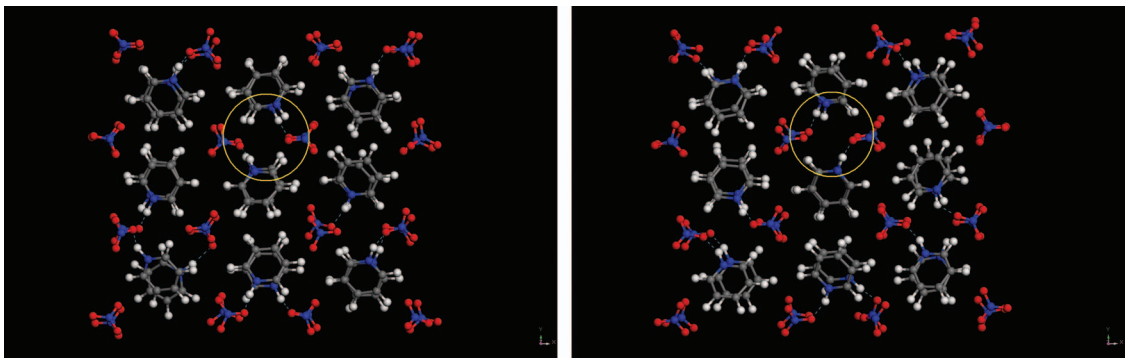

FIG. 7. The snapshots at 290 K for $(PyH)NO_3$ (two layers of pyridinium cations and nitrate anions), time step 1.5 ps. The hydrogen bonds are depicted as blue, dotted line. Comparing two picture is easily to see that the jump of pyridinium cation by 60° is followed by the formation of hydrogen bond with another nitrate anion.

$EISF_{experim} = A_0(Q)$ in a model independent way. Figure 6 shows a representative example of a QENS spectrum and the fit obtained with Eq. (1) for $Q = 1.6$ Å^{-1}, together with the experimental $EISF_{experim} = A_0(Q)$obtained from such fit. The EISF obtained from the MD simulation is also plotted in this figure, showing a good agreement with the QENS result.

Previous NMR measurements are also consistent with the picture of the pyridinium cation performing reorientations between inequivalent positions in $(PyH)NO_3$. However, in Ref. 3 the reorientations were assumed to take place between six positions, while the present QENS and MD results seem to indicate that only two orientations are significantly populated.

The analysis of several of the configurations obtained during the MD trajectory (see Fig. 7) shows the presence of the N–H$\cdots$O hydrogen bond between the cation and the nitrate anion. In Fig. 7, two neighbouring snapshots are presented and the hydrogen bond is depicted as a blue line. Comparing two snapshots is easily to see that several pyridinium cations jumped by 60° (one example is in a yellow circle). Such jump is followed by the formation of the hydrogen bond with another nitrate anion. Therefore, we can say that two positions, which are populated, are connected with HBs and other 4 are not occupied because in that case the formation of the hydrogen bond is not possible. The evolution of this H-bond with temperature has been followed by computing the average distance between H and O and the angle between the vectors N–H and H–O during the MD trajectory. The results are shown in Fig. 8, together with experimental values obtained from X-ray diffraction.[28] In the range 100–150 K, the length and angle do not change and are approximately equal to 1.7 Å and 164°, respectively. With increasing temperature the hydrogen bond length increases up to 2 Å at 390 K, while the average angle N–H$\cdots$O decreases down to 145°. The simulated lengths are in very good agreement with the experimental data and indicate that with increasing temperature hydrogen bonds become weaker.

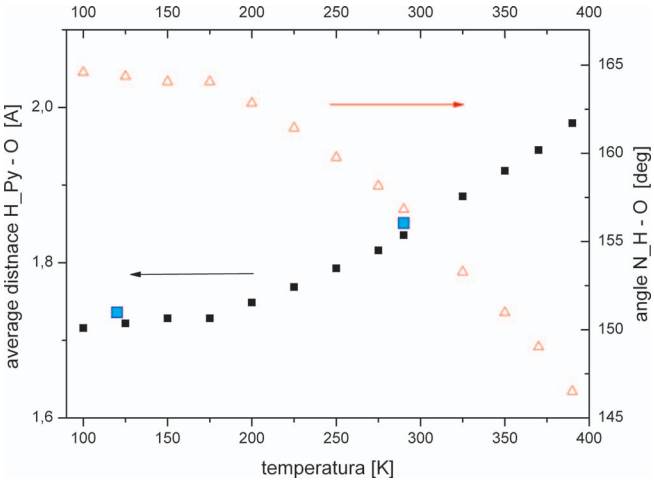

FIG. 8. The average distance between hydrogen atom (in pyridinium cation attached to nitrogen) and oxygen atom in nitrate anion (left, black square – MD simulations, blue square – the experimental values [Ref. 28]), the angle between nitrogen, hydrogen and oxygen (right).

According to the MD simulations, at room temperature the pyridinium cation in $(PyH)NO_3$ can take two positions of different probability of population, which suggests a two-well potential. It can be characterized by the energy E_b (the depth of the less populated well), energy E_a (the depth of the more populated well), and the parameter Δ defined as the difference $E_a - E_b$. The value of Δ was found experimentally on the basis of the temperature dependence of the second moment of the NMR line.[3] The authors of Ref. 3 have shown that only assuming a temperature dependence in Δ is possible to describe correctly the changes in the second moment M_2. As mentioned above, these authors applied a six-well model. Using the same experimental M_2 data but assuming the model of jumps between two inequivalent positions described in Ref. 42 the experimental value of Δ_{exp} was determined for the temperature dependent model.

Changes in the occupation probability of the two positions were also followed in the MD simulations as a function of temperature. At the lowest temperature studied (100 K) only one position (0°) is populated, while with increasing temperature the population of position 1 (0°), denoted as p_1, decreases, while that of position 2 (60°), denoted as p_2, increases. The parameter Δ is defined as the ratio of populations between these two positions: $p_1/p_2 = \exp(\Delta/RT)$ (where R is the gas constant and T is the temperature). Using this equation, we can use the values of p_1 and p_2 obtained from the MD simulations at different temperatures to compute Δ_{sim}. In order to normalize Δ_{sim} we assumed that at the lowest temperatures (100 K) $\Delta_{sim} = \Delta_{exp}$. Figure 9 compares the

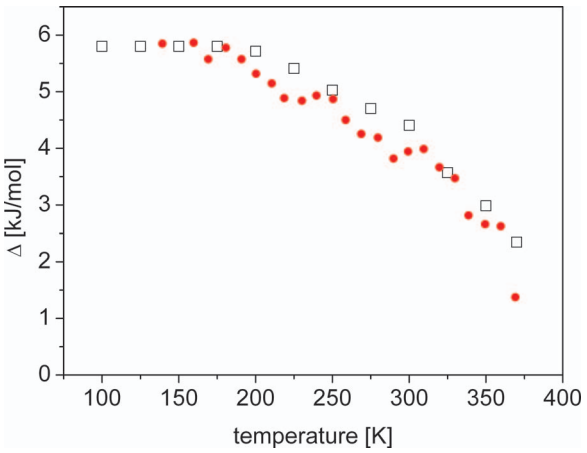

FIG. 9. Comparison of the experimental parameter Δ extracted from Ref. 3 (●) with the simulated one (□) for $(PyH)NO_3$.

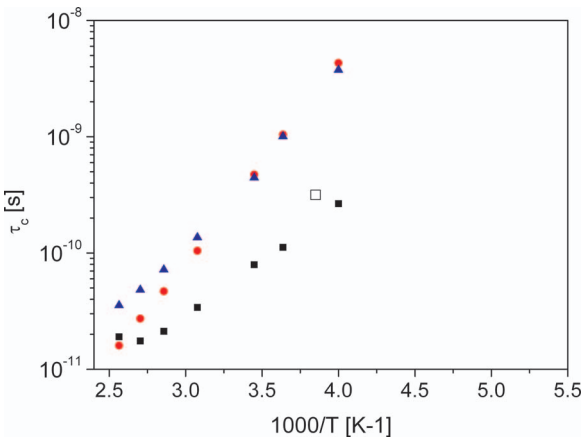

FIG. 10. The correlation time: simulated for (■) piridinium cation in $(PyH)NO_3$, (▲) nitrate anion perpendicular to anion plane (●) nitrate anion, in-plane; (□) experimental (QENS data) for pyridinium cation in $(PyH)NO_3$.

experimental and simulated values of the parameter Δ. It is interesting to observe that the temperature at which the parameter Δ starts to change (i.e., at T ∼ 180 K) coincides with the temperature where also the length of the HB bond starts to increase and the N–H···O angle starts to decrease. Therefore, similarly as for the low temperature phase of (PyH)I, also in $(PyH)NO_3$ the pyridinium cation reorientations take place in an asymmetric potential that undergoes changes with temperature. As follows from the MD simulations and from earlier NMR measurements as a function of temperature and pressure,[3,4] with increasing temperature the population of the potential energy minima is gradually equalized. Moreover, starting from 200 K, at which the populations of the two minima of potential energy begin to equalize, the hydrogen bond N–H···O length begins to increase and the N–H···O angle begins to decrease.

In the case of $(PyH)NO_3$, it is important to explore the rotational dynamics of the nitrate anions as well. For this purpose, two vectors were defined, one in the plane of the NO_3^- anion and another perpendicular to it. For these two vectors, the reorientational ACF and their corresponding correlation times were computed as before (Fig. 10). The values of the in- and out-of-plane correlation times coincide in the temperature range 100 K–300 K, but above 300 K the reorientation of the NO_3 anions in the plane becomes faster than that out-of-plane. Additionally, in the whole temperature range studied, the correlation times of the anion are larger than those of the in-plane motion of the cation. Interestingly, with increasing temperature the correlation times characterizing the in-plane reorientations of the pyridinium cation and the nitrate anion converge to a common value. The full convergence occurs at a temperature that coincides with the experimental melting point of this compound. A similar behaviour has been observed experimentally in other ion-molecular systems such as pyridinium tetrafluoroborate,[5] guanidinium tetrafluoroborate,[25] and guanidinium hexafluorophosphate,[26] whose correlation times have been obtained from NMR measurements. For these compounds, the convergence of the correlation times has always been related to phase transitions that take place at the same temperature. A similar behaviour has been observed in some molecular systems where at the phase transition temperature the correlation times describing reorientations of different molecular groups become similar.[43–45] It is worth to mention that the experimental correlation time of in-plane cation's motion obtain directly from width of Lorentzian (Eq. (1)) is in a good agreement with simulated data. We have also analyzed in detail the geometry of motion of nitrate anions. This analysis showed that the potential for out-of-plane reorientation has a twofold symmetry, while the in-plane motion of the NO_3^- anion takes place between three positions (distanced by 120°).

As follows from the analysis of the trajectory frames, at low temperatures the pyridinium cation is linked to only one nitrate anion through a single hydrogen bond. When approaching the melting point the formation of hydrogen bonds of similar lengths between the pyridinium cation and two neighbouring nitrate anions becomes possible. This explains why the populations of positions p_1 and p_2 are comparable. Formation of hydrogen bonds of similar lengths between the pyridinium cation and neighbouring nitrate anions is made possible only by a correlated reorientation of the anions.

B. Simulations as a function of pressure

Pressure is a very important physical parameters which can influence strongly both the structure and dynamics of molecular crystals. Therefore, for the three systems studied (benzene, pyridinium iodide, and pyridinium nitrate), we also performed MD simulations as a function of pressure, going from ambient pressure up to 8 kbar.

As a first test of the validity of the MD simulations, we compared the experimental and simulated compressibilities. From the changes in the elementary cell parameters with pressure obtained from the *NPT* simulations, the compressibility can be calculated from the Birch equation[46]

$$p = \frac{3}{2}B_0\left[\left(\frac{V}{V_0}\right)^{-7/3} - \left(\frac{V}{V_0}\right)^{-5/3}\right] \times \left[1 + \frac{3}{4}(B_1 - 4)\left(\left(\frac{V}{V_0}\right)^{-2/3} - 1\right)\right], \quad (6)$$

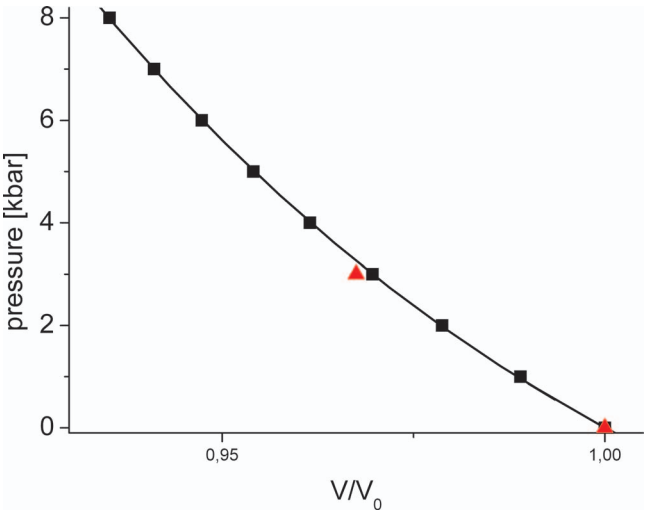

FIG. 11. Pressure dependences of the unit cell volume for $(PyH)NO_3$: (■) simulated, (▲) experimental [Ref. 47]. (Solid line) Fit to the Eq. (4).

where V_0 is the volume at zero pressure, B_0 is the compressibility modulus at zero pressure, and $B_1 = dB_0/dp$. Figure 11 shows the pressure dependence of V/V_0 obtained from the simulations for $(PyH)NO_3$ and compares this with the experimental values available.[47] The values of the compressibility modulus B_0 obtained from the best fit of the Birch equation to the values obtained from the MD simulations are given in Table III for the three compounds and they are compared to literature data.

The same type of analysis of the dynamics of the benzene and pyridinium cations performed before as a function of temperature, was done now as a function of pressure. Again, for benzene and (PyH)I the distribution function $P(\Theta)$ displays six equal maxima, while for $(PyH)NO_3$ there are two nonequal maxima at 0° and 60°. Increasing the pressure did not change the shape of the potential in any of the compounds studied. It is worth to underline that in $(PyH)NO_3$ the probabilities p_1 and p_2 corresponding to the occupation of the positions at 0° and 60° are pressure independent, implying that the parameter Δ_{sim} is not dependent on pressure which is again in good agreement with experimental data.[4] On the other hand, applying pressure influences strongly on the rotational correlation times calculated from the ACF. The analysis of those times as a function of pressure allows to determine the activation volume, ΔV^*. This is usually defined as the change in volume when molecules move from their equilibrium position to the saddle point,[48] and is at least a qualitative parameter characterizing molecular motion. It can be found from the formula

$$\Delta V^* = RT\left[\frac{\partial \ln \tau}{\partial p} + \frac{\partial \ln \nu}{\partial p}\right]_T, \tag{7}$$

where τ is the correlation time and ν is the frequency of crystal lattice vibrations.

In order to determine the first term in Eq. (7) (usually much greater than the second term), the pressure dependence of the correlation times of molecular motions should be found. The MD simulations as a function of pressure provide those times and permit to calculate the activation volume from the slope of their pressure dependence. The values obtained are collected in Table III. For benzene and (PyH)I, the agreement between experiment and simulations is very good, while for $(PyH)NO_3$ the activation volume from the simulation is much higher than the experimental one. The difference can be a result of the fact that for the reorientation between the potential energy minima of different depths Eq. (7) is not appropriate.

For $(PyH)NO_3$, the N–H···O hydrogen bond between the cation and the nitrate anion were analyzed as before. The evolution of this H-bond with pressure has been followed by computing the average distance between H and O and the angle between the vectors N–H and H–O. Interestingly, up to 8 kbar the length and angle do not change and are approximately equal to 1.84 Å and 156°, respectively. Therefore, one can conclude that moderate pressures do not alter significantly the strength of the hydrogen bond in this compound.

V. CONCLUSIONS

The results of MD simulations for benzene, pyridinium iodide, and pyridinium nitrate as a function of temperature and pressure have been compared with the experimental data obtained by NMR and QENS methods, taken from the literature and from new experiments presented in this study.

On the basis of the MD simulation results, the correlation times, activation energies, and geometries of motion were calculated for the benzene molecule and pyridinium cation. In benzene (in the crystal phase) and pyridinium iodide (in HT phase), the molecule/cation performs reorientations between six equivalent positions. In pyridinium nitrate, the geometry of the cation motion is much different, the cation reorients between two inequivalent positions separated by 60°. As follows

TABLE III. Experimental and simulated isothermal compressibility coefficients and activation volumes.

	Isothermal compressibility coefficients [1/GPa] experimental	Isothermal compressibility coefficients [1/GPa] simulated	Activation volume [cm^3/mol] experimental	Activation volume [cm^3/mol] simulation
Benzene	0.148 (T = 270 K) [Ref. 50]	0.209 (T = 270 K)	13.4 (T = 270 K) [Ref. 52]	14.03 (T = 270 K)
(PyH)I	0.150 (T = 300 K) [Ref. 51]	0.145 (T = 300 K)	9.7 (T = 300 K) [Ref. 2]	11.0 (T = 300 K)
$(PyH)NO_3$	0.125 (T = 290 K) [Ref. 47]	0.129 (T = 290 K)	1.4 (T = 290 K) [Ref. 4]	6.85 (T = 290 K)

from the simulations, the cation dynamics in $(PyH)NO_3$ is strongly dependent on the hydrogen bond between the cation and the anion. The nitrate anion was evidenced to perform reorientations in its plane and about perpendicular to its plane. The correlation times were found to converge with increasing temperature.

On the basis of the simulations carried out as a function of pressure it was possible to determine the isothermal compressibility, the geometry of molecule/cation motion, their correlation times and the activation volume. For the three compounds studied, the calculated values of compressibility are in good agreement with the experimental values. A good agreement between the calculated and experimental values of the activation volume was obtained for benzene and pyridinium iodide, while a considerable discrepancy was noted between the experimental and calculated values for pyridinium nitrate. This discrepancy was interpreted as a consequence of the fact that the expression for the activation volume may not be appropriate when the molecular reorientation takes place between inequivalent positions.

MD simulations have also revealed that the effect of temperature in the relative heights of the rotational barriers due to the formation of H-bonds between the pyridinium cation and the anion is much more important than that of the pressure.

ACKNOWLEDGMENTS

This work has been partially financed by the Ministry of Science and Higher Education of Poland, Grant No. 202 032937 and by the operating program POKL 4.1.1.

[1] J. Wąsicki, W. Nawrocik, Z. Pająk, I. Natkaniec, and A. V. Belushkin, Phys. Status Solidi A **114**, 497 (1989).
[2] S. Lewicki, J. Wąsicki, P. Czarnecki, I. Szafraniak, A. Kozak, and Z. Pająk, Mol. Phys. **94**, 973 (1998).
[3] A. Kozak, M. Grottel, J. Wąsicki, and Z. Pająk, Phys. Status Solidi A **143**, 65 (1994).
[4] S. Lewicki, J. Wąsicki, L. Bobrowicz-Sarga, A. Pawlukojc, I. Natkaniec, and A. Kozak, Phase Transitions **76**, 261 (2003).
[5] J. Wąsicki, Z. Pająk, and A. Kozak, Z. Naturforsch. **45a**, 33 (1990).
[6] P. Czarnecki, W. Nawrocik, Z. Pająk, and J. Wąsicki, Phys. Rev. B **49**, 1511 (1994).
[7] P. Czarnecki, W. Nawrocik, Z. Pająk, and J. Wąsicki, J. Phys.: Condens. Matter **6**, 4955 (1994).
[8] P. Czarnecki, J. Wąsicki, Z. Pająk, R. Goc, H. Małuszyńska, and S. Habryło, J. Mol. Struct. **404**, 175 (1997).
[9] Z. Pająk, P. Czarnecki, J. Wąsicki, and W. Nawrocik, J. Chem. Phys. **109**, 6420 (1998).
[10] J. Wąsicki, P. Czarnecki, Z. Pająk, W. Nawrocik, and W. Szczepański, J. Chem. Phys. **107**, 576 (1997).
[11] A. Kozak, M. Grottel, J. Wąsicki, and Z. Pająk, Phys. Status Solidi A **141**, 345–352 (1994).
[12] J. W. Wąsicki, A. Kozak, Z. Pająk, P. Czarnecki, A. V. Belushkin, and M. A. Adams, J. Chem. Phys. **105**, 9470 (1996).
[13] A. Kozak, J. Wąsicki, and Z. Pająk, Phase Transitions **57**, 153 (1996).
[14] J. A. Ripmeester, J. Chem. Phys. **85**, 747 (1986).
[15] J. Ripmeester, Can. J. Chem. **54**, 3453 (1976).
[16] R. Mukhopadhyay, S. Mitra, I. Tsukushi, and S. Ikeda, Chem. Phys. Lett. **341**, 45 (2001).
[17] Z. Fojud, R. Goc, S. Jurga, A. Kozak, and J. Wąsicki, Mol. Phys. **101**, 1469 (2003).
[18] J. Wąsicki, S. Lewicki, P. Czarnecki, C. Ecolivet, and Z. Pająk, Mol. Phys. **98**, 643 (2000).
[19] J. Wąsicki, Z. Fojud, P. Czarnecki, and S. Jurga, Ferroelectrics **368**, 63 (2008).
[20] H. Małuszyńska, P. Czarnecki, S. Lewicki, J. Wąsicki, and M. Gdaniec, J. Phys.: Condens. Matter **13**, 11053 (2001).
[21] L. Bobrowicz-Sarga, P. Czarnecki, S. Lewicki, I. Natkaniec, W. Nawrocik, and J. Wąsicki, Phase Transitions **80**, 725 (2007).
[22] J. Wąsicki, A. Pajzderska, and Z. Fojud, J. Phys. Chem. **112**, 7503 (2008).
[23] P. Czarnecki, A. I. Beskrovny, L. Bobrowicz-Sarga, S. Lewicki, and J. Wąsicki, J. Phys.: Condens. Matter **17**, S3131 (2005).
[24] S. E. Kichanov, D. P. Kozlenko, J. Wasicki, W. Nawrocik, P. Czarnecki, B. N. Savenko, V. P. Glazkov, and C. Lathe, J. Mol. Struct. **875**, 58 (2008).
[25] J. Wąsicki, M. Grottel, A. Kozak, and Z. Pająk, Z. Naturforsch. **47a**, 803 (1992).
[26] M. Grottel, A. Kozak, A. E. Kozioł, and Z. Pająk, J. Phys.: Condens Matter **1**, 7089 (1989).
[27] von Hans Hartl, Acta Crystallogr. **B31**, 1781 (1975).
[28] A. S. Batsanov, Acta Crystallogr. E **60**, o2424 (2004); **60**, o2426 (2004).
[29] G. E. Bacon, N. A. Curry, and S. A. Wilson, Proc. R. Soc. London, Ser. A **279**, 98 (1964).
[30] F. Fujara, W. Petry, W. Schnauss, and H. Sillescu, J. Chem. Phys. **89**, 1801 (1988).
[31] See http://www.ill.eu/instruments-support/computing-for-science/cs-software/all-software/lamp/ for full description of the program.
[32] M. Bee, *Quasielastic Neutron Scattering* (Hilger, Bristol, 1988).
[33] M. Bée, Physica B **182**, 323 (1992).
[34] W. Smith, C. W. Young, and P. M. Rodger, Mol. Simul. **28**, 385 (2002).
[35] A. Pajzderska, M. A. Gonzalez, and J. Wąsicki, J. Chem. Phys. **135**, 074508 (2011).
[36] A. Pajzderska, M. A. Gonzalez, and J. Wąsicki, Phys. Chem. Chem. Phys.**14**, 3949 (2012).
[37] Materials Studio Modelling Environment, Version 5.5, Accelrys, Inc., San Diego, CA, 2009.
[38] E. R. Andrew and R. G. Eads, Proc. R. Soc. London, Ser. A **218**, 537 (1953).
[39] F. Noack, M. Weithase, and J. von Schutz, Z. Naturforsch. **30a**, 1707 (1975).
[40] T. Rog, K. Murzyn, K. Hinsen, and G. R. Kneller, J. Comput. Chem. **24**, 657 (2003), see http://dirac.cnrs-orleans.fr/plone/software/nmoldyn/.
[41] N. D. Morelon, G. R. Kneller, M. Ferrand, A. Grand, J. C. Smith, and M. Bée, J. Chem. Phys. **109**, 2883 (1998).
[42] D. C. Look and I. J. Lowe, J. Chem. Phys. **44**, 2995 (1966).
[43] E. Szcześniak, Mol. Phys. **58**, 551 (1986).
[44] E. Szcześniak, Mol. Phys. **59**, 679 (1986).
[45] N. J. Hess, M. R. Hartman, C. M. Brown, E. Mamontov, A. Karkamkar, D. J. Heldebrant, L. L. Daemen, and T. Autrey, Chem. Phys. Lett. **459**, 85 (2008).
[46] F. Birch, J. Geophys. Res. **83**, 1257, doi:10.1029/JB083iB03p01257 (1978).
[47] D. P. Kozlenko, J. W. Wasicki, V. P. Glazkov, S. E. Kichanov, W. Nawrocik, and B. N. Savenko, Crystallogr. Rep. **50**, 78 (2005).
[48] J. M. Chezeau and J. H. Strange, Phys. Rep. **53**, 1 (1979).
[49] U. Haeberlen and G. Maier, Z. Naturforsch. A **22**, 1236 (1967).
[50] M. M. Thiery and J. M. Leger, J. Chem. Phys. **89**, 4255 (1988).
[51] M. Szafrański and I. Szafraniak, J. Phys.: Condens. Matter **15**, 5933 (2003).
[52] S. McGuigan, J. H. Strange, and J. M. Chezeau, Mol. Phys. **2**, 373 (1982).